Decomposition Pathways and *in Vitro* HIV Inhibitory Effects of IsoddA Pronucleotides: Toward a Rational Approach for Intracellular Delivery of Nucleoside 5′-Monophosphates

Gilles Valette,[†] Alain Pompon,[†] Jean-Luc Girardet,[†] Loredana Cappellacci,[‡] Palmarisa Franchetti,[‡] Mario Grifantini,[‡] Paolo La Colla,[§] Anna Giulia Loi,[§] Christian Périgaud,[†] Gilles Gosselin,[†] and Jean-Louis Imbach*[,†]

Laboratoire de Chimie Bioorganique, URA CNRS 488, case courrier 008, Université Montpellier II, Sciences et Techniques du Languedoc, Place E. Bataillon, 34095 Montpellier Cédex 5, France, Dipartimento di Scienze Chimiche, Università di Camerino, 62032 Camerino, Italy, and Dipartimento di Biologia Sperimentale, Università di Cagliari, 09124 Cagliari, Italy

Received October 4, 1995[⊗]

The decomposition pathways and kinetics in various biological media and the *in vitro* anti-HIV-1 and anti-HIV-2 activities of four derivatives of the 5′-mononucleotide of isoddA incorporating carboxylate esterase-labile transient phosphate protecting groups are reported and compared: namely, two mononucleoside aryl phosphoramidate derivatives **1a**,**b** and two mononucleoside phosphotriester derivatives incorporating two *S*-acyl-2-thioethyl groups **2a**,**b**. All four compounds show better antiviral activity, compared to the parent nucleoside analog isoddA. The results highlight that both types of compounds act as pronucleotides, i.e. they exert their antiviral effect via intracellular delivery of the 5′-mononucleotide of isoddA. The results may give insights for the design of new more efficient pronucleotides.

Introduction

Most of the nucleoside analogs showing antiviral activity need to be phosphorylated to the corresponding triphosphates before exerting their biological effects. In many cases, among the three successive phosphorylation steps, the first is rate limiting, and further conversions to the di- and triphosphates are catalyzed by less specific kinases.[1,2] Therefore, to overcome the first highly selective and regulated phosphorylation step, the use of nucleotide prodrugs (pronucleotides) has been suggested; this could intracellularly deliver the 5′-mononucleotide (NuMP).[1] In this respect, the studies of two types of phosphotriester pronucleotides I and II (Figure 1) which incorporate (pivaloyloxy)methyl (POM)[3] or *S*-acyl-2-thioethyl (SATE)[4,5] groups as enzyme-labile phosphate masking groups have been previously reported.

On the basis of several nucleosidic models, it has been demonstrated that mononucleoside bis(POM) and bis(SATE) phosphotriester derivatives were able to liberate the NuMP inside the cell. For instance, the bis(POM) ester of 2′,3′-dideoxyuridine 5′-monophosphate (type I, Nu = ddU) showed an anti-HIV inhibitory effect in various cell lines,[3a] and bis(POM) derivatives of various acyclic nucleoside phosphonates were found to exhibit antiviral activity greater than their corresponding unmodified compounds.[3b] More recently, it was reported that several bis(SATE) esters of 3′-azido-2′,3′-dideoxythymidine monophosphate (type II, Nu = AZT) showed marked anti-HIV activity in thymidine kinase-deficient (TK^-) cell lines.[4] In addition, the bis(SATE) phosphotriester derivative of 2′,3′-dideoxyadenosine (type II, Nu = ddA, R = CH_3) exhibited the most potent inhibitory effect already described in various HIV-1-infected cell lines with a 50% effective concentration up to 10 pM in monocyte/macrophages.[6]

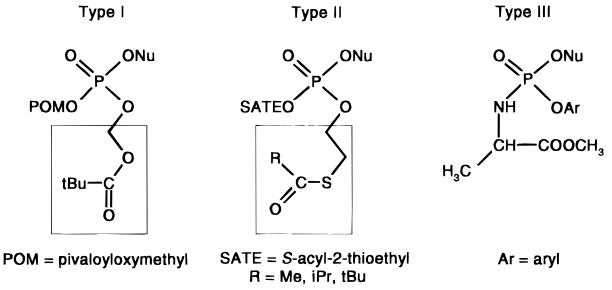

Figure 1. Various types of anti-HIV pronucleotides.

We have previously demonstrated that the mechanism by which the two types of pronucleotides I and II are converted to the NuMP involves, in a first step, a carboxyesterase-mediated decomposition process (Scheme 1) followed by a spontaneous and selective C_α−O bond breakage and thus giving rise to the corresponding phosphodiesters.[4,7] However, the I and II series differ on the nature of the elimination product, i.e. formaldehyde versus episulfide. In a second step, the corresponding phosphodiesters are transformed to the expected NuMP either following a decomposition process similar to that involved in the first step and/or by phosphodiesterase-mediated hydrolysis.

Some aryl phosphoramidate derivatives of 3′-azido-2′,3′-dideoxythymidine (Figure 1, type III, Nu = AZT) have been reported to exhibit anti-HIV activity in TK^- cell lines.[8] Furthermore, the 5′-(phenyl phosphoramidate) derivative **1a** of 2′,3′-dideoxy-3′-oxoadenosine (Figure 1, type III, Nu = isoddA, Ar = phenyl) was at least 100 times more effective than the parent nucleoside isoddA in cell culture assays.[9] However, the mechanisms involved in the antiviral activity of these compounds remains unknown. In order to determine if such phosphoramidate derivatives exert their biological effects via intracellular delivery of the corresponding NuMP, we decided to establish the decomposition

* Corresponding author. Tel: (33) 67 41 25 30; Fax: (33) 67 04 20 29.
[†] Université Montpellier II.
[‡] Università di Camerino.
[§] Università di Cagliari.
[⊗] Abstract published in *Advance ACS Abstracts,* April 1, 1996.

S0022-2623(95)00733-3 CCC: $12.00

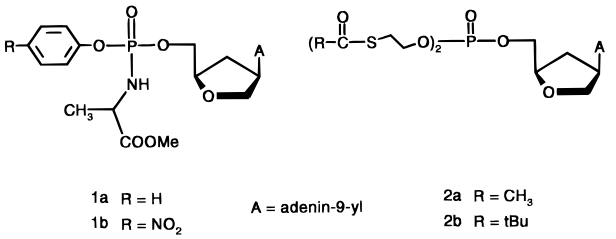

Figure 2. Structure of the studied pronucleotides of isoddA.

Scheme 1. Decomposition Pathways of Types I and II Pronucleotides in Full CEM Cell Extract

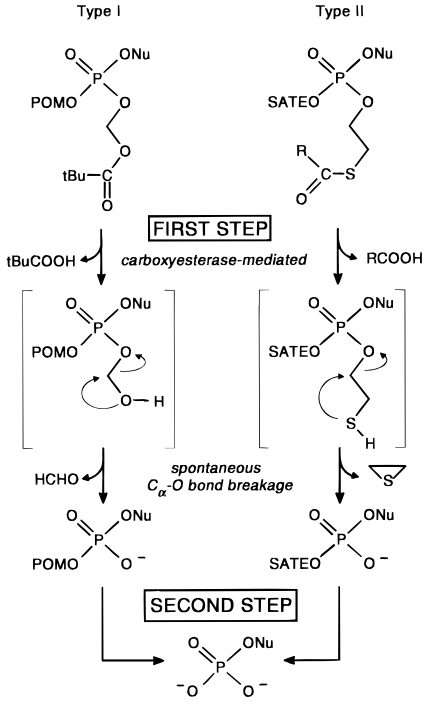

pathways of **1a** and its *p*-nitrophenyl analog **1b** (Figure 2) in a full cell extract as well as to determine their stability in other various media. We have also synthesized two bis(SATE) phosphotriester derivatives **2a**,**b** (Figure 2) in order to compare (i) the decomposition kinetics in the same biological media and (ii) the *in vitro* anti-HIV efficacy of the four isoddA nucleotide derivatives **1a**,**b** and **2a**,**b**.

Chemistry

The 5′-(phenyl phosphoramidate) derivative of isoddA **1a** was prepared as previously described,[9] and a similar synthetic strategy was used in the preparation of the hitherto unknown *p*-nitrophenyl analog **1b**. Coupling of isoddA with [(*p*-nitrophenyl)methoxy]alaninyl phosphorochloridate in tetrahydrofuran in the presence of *N*-methylimidazole gave compound **1b** in 45% yield. As anticipated, each compound **1a** and **1b** displayed two closely-spaced signals in the ^{31}P NMR spectrum corresponding to the two diastereoisomers about the phosphate center. The diastereoisomeric mixtures were obtained in a 1:1 ratio as determined by HPLC. The reference phosphoramidate monoester derivatives **3** and **4** were prepared from **1b** under controlled hydrolysis conditions in aqueous triethylamine solutions (Scheme 2).

The hitherto unknown bis(SATE) phosphotriester derivatives of isoddA **2a**,**b** were obtained according to a procedure recently reported in other nucleoside analog series.[4] Coupling of isoddA, in the presence of 1*H*-tetrazole, with appropriate phosphoramidite reagents which incorporate the SATE groups, followed by *in situ* oxydation with *tert*-butyl hydroperoxide, gave the pronucleotides **2a**,**b** in 58 and 80% yields, respectively (Scheme 3).

Scheme 2. Decomposition of **1b** in Triethylamine/Water Solutions[a]

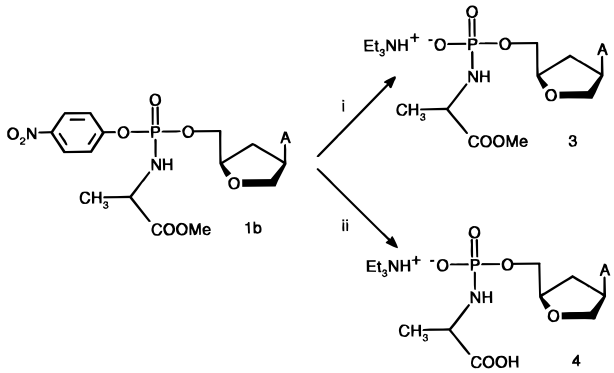

[a] (i) Et_3N (97)/H_2O (3) (v/v), room temperature, 1.5 h; (ii) Et_3N (50)/H_2O (50) (v/v), 40 °C, 2 h.

Scheme 3. Synthesis of Bis(SATE) Phosphotriester Derivatives (**2a**,**b**) of isoddA[a]

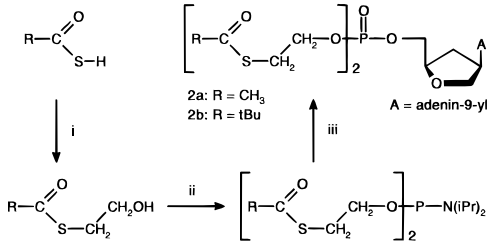

[a] (i) ICH_2CH_2OH, DBU/$C_6H_5CH_3$; (ii) $Cl_2PN(iPr)_2$, NEt_3/THF; (iii) isoddA, 1*H*-tetrazole/THF, then $(CH_3)_3COOH/C_6H_5CH_3$.

Decomposition Studies

The decomposition products, pathways, and kinetics of compounds **1a**,**b** and **2a**,**b** were determined upon incubation (37 °C, initial concentration 25 μM) in a culture medium (RPMI 1640 containing 10% of heat-inactivated fetal calf serum) and in a full CEM cell extract in order to mimic their behavior under the experimental conditions of the *in vitro* assays. Compound **1a** was also incubated in phosphate buffer with or without addition of purified pig liver carboxyesterases and compounds **1a**,**b** in freshly withdrawn human serum. Additionally, the phosphoramidate monoester derivatives **3** and **4** were incubated in cell extract.

During incubation, aliquots were removed and analyzed using a recently improved "on-line cleaning" method which allows the direct HPLC analysis of drugs and metabolites in biological samples without any pretreatement.[4,7] Briefly, samples were deproteinized by means of a cleaning precolumn which was equilibrated either with an ammonium acetate buffer or with a tetrabutylammonium sulfate buffer (ion-pairing reagent). In both buffers, proteins and other unwanted components were quickly eliminated. The very hydrophilic anionic species were also quickly eluted on the precolumn in the first case, but were ion-paired and retained in the second. Conversely, the final decomposition product, namely isoddA, was retained in the first case, but quickly eluted in the second, due to the increased lipophilicity of the eluent. Whatever the

technique, phenol (from the decomposition of **1a**) was quickly eliminated, while *p*-nitrophenol (from the decomposition of **1b**) was retained on the precolumn. For both techniques, the trapped analytes were then transferred by means of a switching device onto an RP (C_{18}) analytical column (acetonitrile gradient) and analyzed (UV diode-array detection). When the results obtained with both techniques were combined, all the starting compounds and the corresponding metabolites could be accurately UV-detected and quantified. All the aforementioned assumptions were confirmed by injection of authentic samples.

Decomposition Studies of Aryl Phosphoramidate Derivatives 1a,b. After incubation of **1a** in the various investigated media, aliquots were HPLC-analyzed and several signals could be observed in the resultant chromatograms. Four of them were unambiguously assigned by co-injection with authentic samples (retention time, UV spectra) to the starting material **1a** (two diastereoisomers), the 5′-mononucleotide of isoddA (isoddAMP), and the parent nucleoside (isoddA). According to the medium, one or two additional signals were observed but, due to the similarity of all UV spectra, it was impossible to ascertain the structure of the corresponding compounds. In contrast, the UV spectrum of the *p*-nitrophenyl analog **1b** (two diastereoisomers) was quite different than those of all the signals observed during its incubation in the investigated media. Furthermore, in each medium, these signals corresponded (retention time and UV spectra) to those found for the decomposition of **1a** which indicated that all observed metabolites lacked the aromatic moiety.

On the basis of our previous study[7] and literature data,[10] the degradation of **1a**,**b** may involve two competitive mechanisms (Scheme 4) initiated either by a nucleophilic attack on the phosphorus atom (path A) or by hydrolysis of the acyl moiety (path B).

In order to verify these assumptions, we unequivocally synthesized the corresponding phosphoramidate monoesters **3** and **4**. These compounds exhibited retention times and UV spectra identical to the unknown signals observed in the decomposition of **1a**,**b**. Assuming the hypothetical decomposition pathway described on Scheme 4, the formation of **4** from **1a**,**b** through a carboxyesterase activation (path B) may imply the existence of the transient intermediates **5a**,**b** and **6**. From the cyclic mixed anhydride **6**, P−O or P−N bond cleavage may be envisaged,[10] giving rise to the isomeric compounds **4** or **7**, respectively. One could not exclude the fact that **6** or **7** has chromatographic properties very close to those of **4**, and that these compounds could be co-eluted, thus providing a misinterpretation in the assignment of HPLC signals. In order to investigate this hypothesis, LC/MS coupling experiments were performed. A mixture of incubates in cell extract and in culture medium of compound **1b** (which contained all the degradation products) was on-line cleaned with the ion-pairing conditions, then transferred into the column, and analyzed by both UV detector and mass spectrometer (electrospray or API sources in negative or positive modes). The pseudo-molecular masses ($[M-H]^-$or $[M+H]^+$) of all the observed compounds corresponded respectively to the expected structures of **1b**, **3**, **8**, *p*-nitrophenol, and to the isomeric structures of **4** or **7**. With regard to this last component ($[M-H]^-$ = 385.1), a fragment at m/z = 339.1 was observed when increasing the ionization conditions. This fragment is in accordance with the the loss of formic acid (MW = 46) from structure **4**, but could not arise from **7**. In addition, a reconstituted aqueous mixture of **1b**, **3**, **4**, **8**, **9**, and *p*-nitrophenol was directly injected into the analytical column and HPLC/UV/MS analyzed, confirming the assignment of all species obtained from biological samples. Signals corresponding to the structures **5** and **6** were never detected in the incubated samples, but this fact did not exclude their existence as transient intermediates. To our knowledge, the coupling of an "on-line cleaning HPLC" method with both UV and mass detection is the first report of HPLC/UV/MS coupling including the direct analysis of metabolites in crude biological samples without any sample preparation.

Scheme 4. Possible Mechanisms for the Decomposition of **1a**,**b** (**1a**, **5a**, Ar = C_6H_5; **1b**, **5b**, Ar = *p*-$NO_2C_6H_4$)[a]

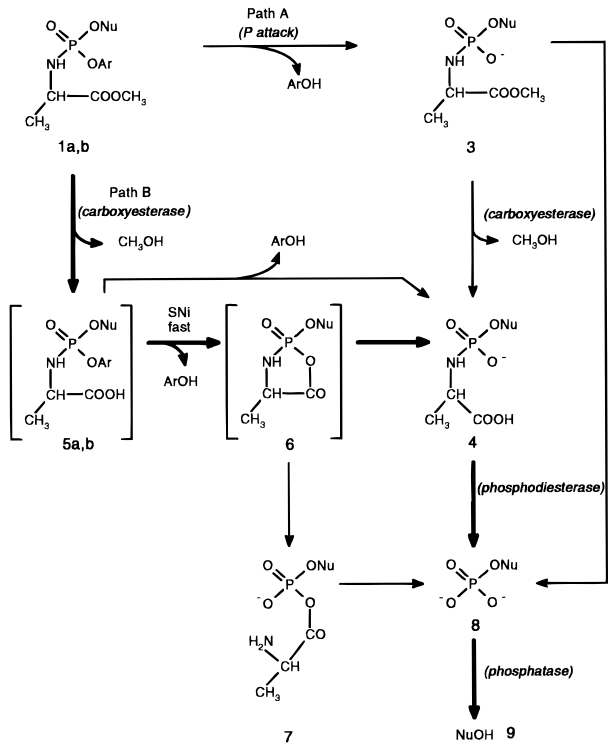

[a] Nu = isoddA in all formulas. In full CEM cell extract, only the pathways in thick arrows were observed. In culture medium and human serum, compound **3** was observed.

Having assigned the various HPLC signals, the kinetic data could be treated according to either a model taking into account a substrate inhibition or a general "consecutive-competitive pseudo-first-order" model. When possible, the rate constants were optimized by mono- or poly-exponential regressions according to integrated equations (Scheme 5). These kinetic models fit the experimental data very accurately ($R > 0.99$ for $N = 10$) which substantiates the reliability of the method.

The calculated half-lives of the starting materials are summarized in Table 1, and the calculated rate constants of each decomposition step in total cell extract are reported in Table 2. The computation of kinetic data of **1a**,**b** decomposition was consistent with mechanisms which differed according to the medium.

In culture medium, the degradation kinetics of each diastereoisomer of **1a** were very similar, but in contrast to our previous results with other nucleotide derivatives,[4,7] they were not in accordance with exponential

Scheme 5. Observed Decomposition Pathways of **2a**,**b** (**2a**, **10a**, **11a**, **13a**, **14a**, R = methyl; **2b**, **10b**, **11b**, R= *tert*-butyl)[a]

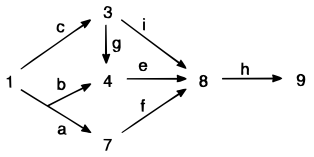

Rate constants: a, b, c, e, f, g, i, h k = a+b+c j = g+i

Parameters: $\alpha = [1]_0/([1]_0+[3]_0) = [1]_0/[\Sigma]$ m = α.c/(j-k) n = α.a/(f-k)

p = (α.b+m.g)/(e-k) q = g.(1-α-m)/(e-j) u = (m.i+n.f+p.e)/(h-k)

v = [q.e+(1-α-m).i]/(h-j) x = n.f/(f-h) y = (p+q).e/(e-h)

Integrated equations (relative concentrations *vs* time):

[**1**]/[Σ] = α.exp(-k.t)

[**3**]/[Σ] = m.exp(-k.t) + (1-α-m).exp(-j.t)

[**7**]/[Σ] = n.[exp(-k.t) - exp(-f.t)]

[**4**]/[Σ] = p.exp(-k.t) + q.exp(-f.t) - (p+q).exp(-e.t)

[**8**]/[Σ] = u.exp(-k.t) + v.exp(-j.t) + x.exp(-f.t) + y.exp(-e.t) - (u+v+x+y).exp(-h.t)

[**9**]/[Σ] = 1 - ([**1**] + [**3**] + [**4**] + [**7**] +[**8**]) / [Σ]

[a] Nu = isoddA in all formulas. In full CEM cell extract the pathways were quite different for the two compounds (see text).

Table 1. Comparative Half-Lives (h) of Compounds **1a**,**b** (25 μM, 37 °C) in Culture Medium, in Human Serum, in Full CEM Cell Extract, and in an Aqueous Buffered Solution of Pig Liver Carboxyesterases (15 units/mL)

	$t_{1/2}$			
compd	culture medium	human serum	CEM cell extract	carboxy-esterase
1a	56	22	1.0	22
1b	14.5	4.3	1.8	ND[a]

[a] ND, not determined.

Table 2. Observed Decomposition Scheme of **1a**,**b** (25 μM, 37 °C) in Full CEM Cell Extract and Calculated Rate Constants (10^{-3} min^{-1}) of Each Step

1 ⟶ **4** ⟶ **8** ⟶ **9**

compd	**1** → **4**	**4** → **8**	**8** → **9**
1a	12.0	1.0	0.75
1b	6.4	1.0	0.80

kinetics (pseudo-first-order process), even when the initial concentration was decreased until the quantification limits. However, the S-shaped curves could be treated according to the substrate inhibition model. Thus, **1a** led mainly to the formation of **4** and **8** with some traces of **3** and **9**. In the same medium, the decomposition pattern of **1b** was similar to that of **1a**, but the first step was faster, giving rise to **3** and **4** at approximately the same rate. Once formed, **3** was slowly decomposed to **4,** which was ultimately decomposed to **8** then **9**. Similar results were obtained when **1a**,**b** were incubated in human serum (example of S-shaped curve on Figure 3), but the half-lives of starting compounds were increased by about 3-fold.

In full CEM cell extract, **1a** and **1b** disappeared much faster than in culture medium or human serum, with concomitant appearence of **4** which reached a maximum at 3−5 h and then decreased to give rise to **8**, which was finally dephosphorylated to the parent nucleoside **9** (Figure 4). In cell extract, **3** was not observed. Data could be treated according to the consecutive−competitive pseudo-first-order model (Scheme 5). The first decomposition step of **1a** or **1b** was initially in good accordance with a first-order process (until 85−90% decomposition) and then deviated from the computed

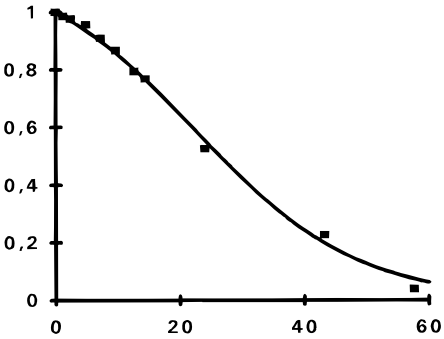

Figure 3. Decomposition kinetics of **1a** (sum of diastereoisomers) at 25 μM; initial concentration in freshly withdrawn human serum. The abcissa shows the incubation time (h) and the ordinate the relative concentration of **1a**. Least-square regression according to substrate inhibition model.

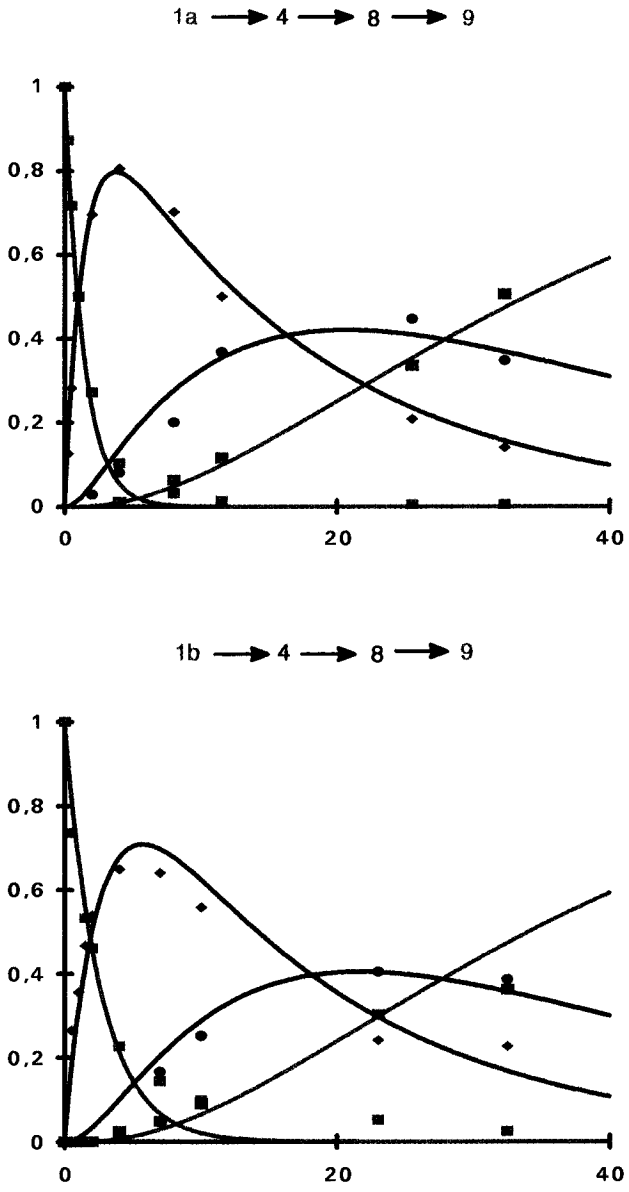

Figure 4. Decomposition kinetics of **1a**,**b** (red squares, sum of diastereoisomers) at 25 μM initial concentration in full CEM cell extract and their degradation products: **4** (blue diamonds), isoddAMP **8** (black circles), and isoddA **9** (magenta squares). The abcissa shows the incubation time (h) and the ordinate the relative concentration of each species. Least-square regression according to the competitive−consecutive pseudo-first-order kinetic model reported in Scheme 5.

exponential curve. This could be tentatively explained by some enzyme inhibition due to the release of phenol

or nitrophenol. Despite this limitation, approximate rate constants could be calculated for each subsequent degradation step (Table 2).

In order to evaluate the various pathways involved in the intracellular formation of **8** from **1a**,**b**, four other experiments were realized: (i) when incubated in full cell extract, an authentic sample of **3** was only slowly decomposed to **4** (rate constant 0.3×10^{-3} min^{-1}), and then to **8**, which may indicate that this phosphoramidate monoester is not a good substrate for cellular carboxyesterases (perhaps due to its bearing a negative charge) nor for cellular phosphodiesterases; this experiment proved that, in cell extract, a nucleophilic attack of **1a**,**b** on the phosphorus atom (Scheme 4, path A) was not the preferential pathway involved in the fast appearance of **4**; otherwise **3** would also be observed; (ii) when a mixture of **1b** and **3** was incubated in total cell extract, the calculated kinetic parameters (data not shown) were in complete accordance with those found in the independant studies of **1b** and **3**; (iii) when **1a** was incubated in phosphate buffer with or without the presence of 15 unit/mL of pig liver carboxyesterase, it gave rise to **4** (Table 1) and traces of **3** in the first case, while it was only very slowly converted to **3** in the second case (data not shown); these results clearly indicate that in enzyme-containing media, the formation of **4** from **1a**,**b** involved mainly, in a first step, a carboxyesterase-mediated decomposition process (Scheme 4, path B); (iv) when an authentic sample of **4** was incubated in total cell extract, the decomposition rate constant (**4** → **8**: 0.97×10^{-3} min^{-1}) was in complete accordance with that found when starting from **1a**,**b** (Table 2); this result definitely excludes the participation of intermediate **7** in the formation of isoddAMP from **1a**,**b**.

In summary, this study allows us to propose a coherent decomposition scheme for pronucleotides of type III (Scheme 4). In cell extract, neutral compounds **1a**,**b** are readily transformed to **4**. Very likely, this transformation occurs upon carboxyesterase activation to the corresponding acids **5a**,**b** which are too unstable to be detected. The great instability of intermediates **5a**,**b** can be difficultly explained by a nucleophilic attack of water on the phosphorus atom to give directly **4**; this would be in contradiction with the stability of **1a**,**b** toward such an attack. Much more likely, the fast transformation of **5a**,**b** to **4** occurs via the unstable mixed cyclic anhydride **6** resulting from an internal nucleophilic substitution with concomitant phenol or *p*-nitrophenol elimination. Therefore, it appears that the P−O cyclic bond cleavage in compound **6** is much faster than the P−N bond cleavage,[10] probably because of the close proximity of the carbonyl group. In turn, **4** is degraded to isoddAMP **8**. In this respect, P−N bonds are known to be stable in neutral aqueous medium;[10] therefore one must assume that this step is enzyme-mediated (likely by phosphodiesterases). Finally, **8** is dephosphorylated to the parent nucleoside **9**, this step is likely phosphatase-mediated as in the case of other nucleotides.[4−7] In culture medium or in human serum, the same degradation pathway is observed, but the carboxyesterase-controlled steps are significantly slower. From this fact, and especially in the case of the *p*-nitrophenyl derivative, a secondary decomposition pathway is brought to the fore (nucleophilic attack on the phosphorus atom, path A), which also gives rise to **4** then **8** and **9** via the relatively stable phosphoramidate monoester **3**.

Table 3. Comparative Half-Lives (h) of Compounds **2a**,**b** and Their AZT Analogs (25 μM, 37 °C) in Culture Medium and in Full CEM Cell Extract

compd	$t_{1/2}$ culture medium	$t_{1/2}$ CEM cell extract
2a	8.3	0.3
2b	120	4.3
bis(MeSATE)AZTMP[a]	9.0	<0.1
bis(*t*-BuSATE)AZTMP[a]	103	1.0

[a] Data from ref 4.

Scheme 6. Decomposition of Type III Pronucleotides[a]

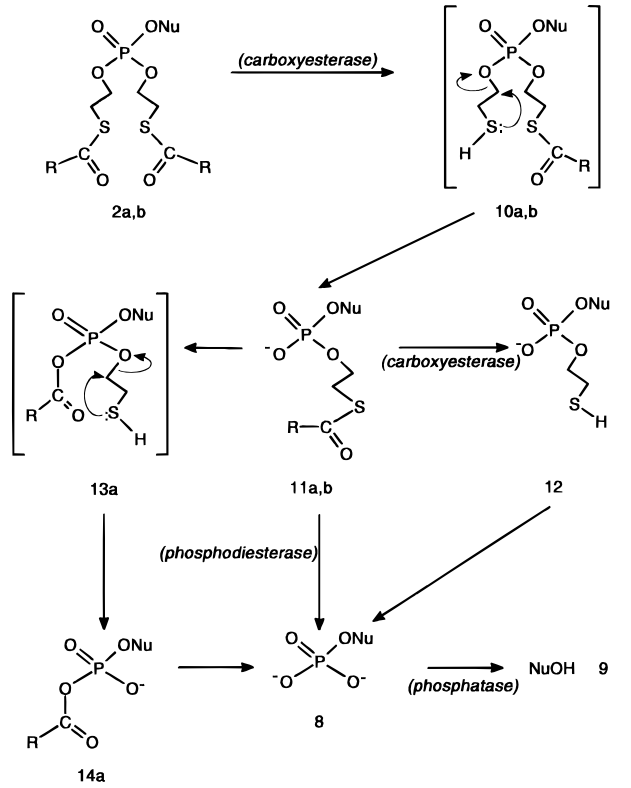

[a] Integrated equations according to the overall competitive consecutive pseudo-first-order kinetic scheme of decomposition of the pronucleotides **1a**,**b** (if the initial sample is not mixed with **3**, let $\alpha = 1$).

Decomposition Studies of the Bis(SATE) Phosphotriester Derivatives 2a,b. In order to get an informative comparison of the pronucleotides of types II and III (Figure 1) we checked the decomposition pattern of the bis(SATE) phosphotriester derivatives **2a** and **2b** in the same full cell extract and culture medium as for the arylphosporamidate derivatives **1a**,**b**. As expected, the rate of the first degradation step of the isoddA derivatives **2a**,**b** was of the same order of magnitude (fast for the methyl derivative, slow for the *tert*-butyl derivative) than those recently published [4] for the corresponding AZT analogs (Table 3). But, unexpectedly, the subsequent degradation patterns were quite different.

In the case of **2a**, a new signal was observed both in cell extract and in culture medium, which indicated a secondary pathway. The corresponding compound was ascertained as intermediate **14a** (Scheme 6) by using the aforementioned LC/MS coupling method. The appearance of this intermediate may be tentatively explained as originating from an unstable phosphotriester **13a** formed by intramolecular (PO^- nucleophilic attack

Table 4. Observed Decomposition Scheme of **2a**,**b** (25 μM, 37 °C) in Full CEM CEll Extract and Calculated Rate Constants (10^{-3} min^{-1}) of Each Step

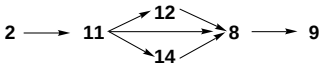

compd	2 → 11	11 → 12	11 → 14	11 → 8	12 → 8	14 → 8
2a	37.0	10.0	8.0	0	4.3	5.7
2b	2.7	0	0	0.12		

Table 5. Comparative Anti-HIV Activity and Cytotoxicity of IsoddA and Its Pronucleotide Derivatives **1a**,**b** and **2a**,**b**

	HIV-1[a]			HIV-2[b]		
compd	EC_{50}[c]	CC_{50}[d]	SI[e]	EC_{50}[c]	CC_{50}[d]	SI[e]
isoddA	45	>450	>10	105	>450	>4
1a	0.1	2.4	24	2.8	62	22
1b	0.22	6	27	3	24	8
2a	0.12	2	17	0.37	13	35
2b	0.09	0.7	8	0.25	5	20
AZT[f]	0.005	150	30000	0.006	>500	>83000
bis(*t*-BuSATE)-ddAMP[f]	0.009	5.4	600	0.02	4.9	245

[a] MT-4 cells acutely infected with HIV-1 strain III_B. [b] C8166 cells acutely infected with HIV-2 strain CBL-20. [c] Compound dose (μM) required to achieve 50% protection of cells from HIV-1 and HIV-2 induced cytopathogenicity, as determined by the MTT assay. [d] Compound dose (μM) required to reduce the viability of mock-infected cells by 50% at day 4, as determined by the MTT assay. [c,d] Values are the mean of three independent determinations. Variation among duplicate samples was <22%. [e] Selectivity index: ratio CC_{50}/EC_{50}. [f] Reference compounds.

on the sp^2-hybridized C atom) or eventually by intermolecular isomerisation of **11a**. In our previous study[4] on the AZT analog of **2a**, we brought to the fore the existence of an unknown intermediate but at trace level. Very likely, this intermediate was the AZT analog of **14a**. This means that the importance of this second pathway strongly depends on the nature of the nucleoside part, probably on the nature of the sugar moiety.

The degradation of **2b** in cell extract was even more unexpected, compared to the results previously obtained when studying the AZT analog of **2b**, for which one observed the AZT analogs of **11b**, **12**, **8**, and **9**.[4] In the present study, the only observed signals corresponded to **11b**, **8**, and **9** without the appearance of compound **12**. Therefore, in contrast with its AZT analog, the isoddA diester derivative **11b** may not be substrate for carboxyesterases. Furthermore, unlike its methyl analog **11a**, the *tert*-butyl derivative **11b** cannot rearrange to give **14b**. Both effects are presumably due to the more important steric hindrance and/or inductive effect introduced by the *tert*-butyl group. The conversion of **11b** to isoddAMP **8** was very slow, likely due to weak phosphodiesterase activity in cell extract. HPLC data were treated according to a "consecutive−competitive pseudo-first-order" kinetic model corresponding to the general decomposition pattern proposed in Scheme 6 (integrated equations were as previously reported[4]). Kinetic parameters are reported in Table 4. Examples of computed kinetic curves are presented in Figure 5.

Antiviral Activity

The pronucleotides of isoddA **1a**,**b** and **2a**,**b** were comparatively evaluated *in vitro* for cytotoxicity and inhibition of the replication of HIV-1 and HIV-2 in MT-4 and C8166 cells, respectively (Table 5). In addition to the parent nucleoside isoddA, two reference compounds were included, namely AZT and the bis(*t*-BuSATE)-ddAMP pronucleotide.[6]

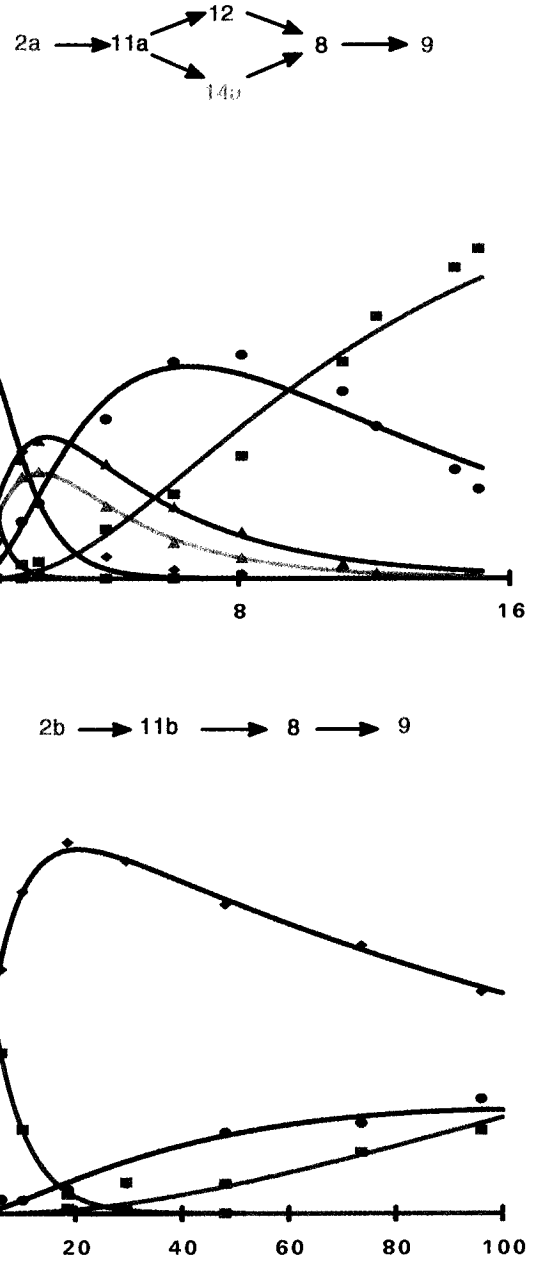

Figure 5. Decomposition kinetics of **2a**,**b** (red squares) at 25 μM initial concentration in full CEM cell extract and their degradation products: **11a**,**b** (blue diamonds), **12** (green triangles), **14a** (cyan triangles), isoddAMP **8** (black circles), and isoddA **9** (magenta squares). Coordinates as in Figure 4. Least-square regression according to the competitive-consecutive pseudo-first-order kinetic model corresponding to Scheme 4. Integrated equations were as previously reported.[4]

The isoddA pronucleotides **1a**,**b** and **2a**,**b** were active against HIV-1 (EC_{50} = 0.09−0.22 μM), and when compared to the parent nucleoside, they were up to 450 times more potent. It is noteworthy that the bis(SATE) derivatives **2a**,**b** are significantly more potent inhibitors of the HIV-2 replication than the phosphoramidate derivatives **1a**,**b**. Moreover, when compared to isoddA, their efficacy is increased by a factor of 280 and 420, respectively. However, all pronucleotides are less active than the reference compounds AZT and bis(*t*-BuSATE)-ddAMP. The latter finding may not be surprising because ddATP is known to be a better inhibitor of the HIV-1 recombinant reverse transcriptase than isoddATP.[9] Compared to isoddA, all pronucleotides show a net increase in cytotoxicity. That may be due to higher intracellular uptake of the prodrugs and subsequent

increased levels of the phosphorylated metabolites. But this remains to be proven.

Discussion

It is evident from the above data as well as from our previous reports[4−7] that the first activation step for series I−III pronucleotides in serum-containing media or in full cell extracts is mainly carboxyesterase-mediated. Carboxyesterases are proteins able to catalyze the hydrolysis of carboxy esters and related compounds, e.g. carboxy thioesters. Although carboxyesterase is a collective term, the related enzymes can be classified into various groups which possess different substrate specificity.[11−13] Such enzymes are widely distributed in mammals from cells to serum. Many carboxyesterases have a serine residue in their active site and have a preference for lipophilic substrates as compared to polar or charged ones.[11−13] As individual esterases differ in their specificities for hydrolysis, each substrate will present different hydrolyzing capacities even if subtle structural changes are involved. For instance, Rp and Sp methyl phosphonothioates present an enantiomeric dependance on their hydrolysis rate.[14,15] Each pronucleotide of type I-III will be activated according to its relative overall substrate capacity towards carboxyesterases and that will determine the rate of the first activation step. The pronucleotide approach needs both the stability of pronucleotides in extracellular media and their instability after uptake in cells, with a view to intracellularly deliver the nucleoside monophosphate. Such a strategy presumes important differences in the carboxyesterase content of extra- and intracellular media.

It appeared from our first study [7] on a pronucleotide of type I (Scheme 1) that the carboxyesterase activities are more important in intracellular medium than in culture medium. This assumption was further confirmed in the case of type II pronucleotides of AZTMP.[4] Moreover the corresponding studies showed that the rate of enzymatic hydrolysis in cell culture medium or freshly withdrawn human serum and the rate of delivery of nucleoside monophosphate in full cell extract could be controlled according to the nature of the acyl group, the more sterically hindered undergoing only slow hydrolysis. The present study confirms these assumptions in the case of other pronucleotides of type II and affords new elements on the decomposition mechanism of this type of prodrug. As expected, the bulky lipophilic *tert*-butyl derivative **2b** is much more stable than the methyl one **2a**. In cell culture medium, the half-lives of isoddA derivatives **2a**,**b** are quite similar to those previously found for their AZT derivative analogs (Table 3). Conversely, in total cell extract, isoddA derivatives are significantly more stable than their AZT analogs (Table 3). Such an increased stability is also observed in cell extract for the diesters **11a**,**b** toward their AZT analogs (respectively 38 min vs <5 min and 96 h vs 7.2 h).[4] It is interesting to observe that diesters of type **11** can be transformed to the nucleoside monophosphate according to three different pathways (Scheme 6): (i) carboxyesterase activation giving rise to a diester of type **12**, which in turn gives NuMP; (ii) isomerization giving rise to a mixed anhydride of type **14**, which in turn gives also NuMP; and (iii) direct hydrolysis to NuMP, likely phosphodiesterase-mediated. The relative importance of these three pathways strongly depends on the nature, lipophilicity, and steric hindrance of the acyl group as well as on the nature of the nucleoside moiety. All these parameters determine the rate of NuMP delivery in cell extracts and presumably in intact cells.

The present study also allowed to determine the decomposition pathways of pronucleotides of type III (Scheme 4). The carboxyesterase-mediated decomposition of compound **1a** has been preliminary confirmed by incubation in the presence of porcine liver esterases (a mixture of seven isoenzymes). Another pathway was brought to the fore, corresponding to a nucleophilic attack on the phosphorus atom. These two pathways give rise to the same phosphoramidate monoester **4** which in turn is transformed into isoddAMP and then into isoddA. When comparing the stabilities of the phenyl (**1a**) and *p*-nitrophenyl (**1b**) derivatives, two effects are observed due to the increased polarity of the last group (Table 1): (i) in culture medium and in human serum where carboxyesterase activities are reduced, the *p*-nitrophenyl derivative is less stable than the phenyl one, due to a preferential nucleophilic attack on the phosphorus atom (respective pK_a 7.16 and 9.9); (ii) conversely, in the cell extract where the carboxyesterase activity is important, thus determining the preferential pathway, the *p*-nitrophenyl derivative is about two times more stable than the phenyl analog, likely due to the weaker affinity of the more polar compound for carboxyesterases. Both compounds are much more stable in culture medium and in human serum than in cell extract, in which the nucleoside monophosphate is easily delivered, both facts being prerequisites for a pronucleotide approach. Phenyl derivatives seem better candidates for such an approach than *p*-nitrophenyl derivatives, due to their higher stability in extracellular media and faster delivery of nucleoside monophosphate in cell extract.

The comparison of kinetic data and anti-HIV *in vitro* assays of compounds of compound types I−III allows interesting insights in the pronucleotide approach. Once activated by carboxyesterases, compounds of types I−III are metabolized through two different mechanisms involving either a C−O (types I and II, Scheme 1) or a P−O (type III, Scheme 4) bond breakage. In the last case the decomposition proceeds through an intramolecular nucleophilic attack of the hard carboxylic oxygen on the phosphorus atom which implies that type III compounds must be substituted with a good leaving group (phenyl for **1a** and *p*-nitrophenyl for **1b**, respectively). Such anchimeric assistance in deplacing a leaving group from phosphorus is well established and involves a pentacoordinate intermediate.[10] The fact that, in order to be metabolized, type III compounds have to bear a good leaving group may present some consequences in terms of stability, and the corresponding elimination product may interfere with the processing carboxyesterases (as suggested by our kinetic data, see Figure 3). It is also pertinent to mention that many esterases, especially serine proteases such as acetylcholine esterase, are inhibited by organophosphorus compounds substituted with good leaving groups,[11−13] and that may give rise to unwanted side effects.[16]

Once formed, the phosphodiesters (Scheme 1, second step) and the phosphoramidate monoester **4** (Scheme 4) are hydrolyzed to the expected NuMP. For compounds of types I and II, this second bioactivation step may follow different enzymatic processes depending on

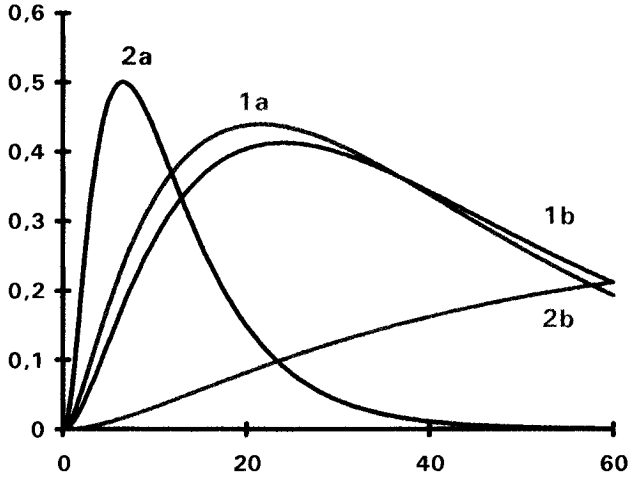

Figure 6. Comparative kinetic release of isoddAMP **8** in full CEM cell extract from **1a**,**b** and **2a**,**b**. The abcissa shows the incubation time (h) and the ordinate the relative concentration of **8**.

the relative affinity of the resulting phosphodiester substrate for carboxyesterases and/or phosphodiesterases. For type I compounds this transformation was shown to be phosphodiesterase-mediated.[7] However for type II compounds this hydrolysis may be carboxyesterase mediated, but at a slower rate than the first decomposition step, presumably because a charged diester has a lower affinity for the enzyme than the starting phosphotriester. In some cases, the phosphodiester may not be substrate for the carboxyesterases [as for the *t*-Bu(SATE) derivative **11b** of isoddAMP, or the mono[(pivaloyloxy)methyl] derivative of AZTMP previously studied[7]], and the hydrolysis may proceed through phosphodiesterases. In other cases (for instance **11a**), a third pathway is brought to the fore that is not enzyme-induced but involves the formation of a mixed anhydride which depends on the steric hindrance of the protecting group and on the nature of the nucleoside analog.

For compounds of type III, the second step is likely phosphodiesterase-mediated. Notably, the esterified phosphoramidate monoester **3** is much more stable toward such hydrolysis in cell extract than the deesterified analog **4** (Scheme 4).

The stability in the culture medium of the four evaluated pronucleotides (8.3 $h < T_{1/2} < 120$ h) seems to be sufficient to permit their quantitative cell uptake during the *in vitro* assays and this is corroborated with their anti-HIV activity. There does not seem any evident correlation between the kinetics of delivery of nucleoside monophosphate in cell extract and the *in vitro* activity; as shown on Figure 6, the rates of isoddAMP delivery are quite different when starting from **1a**,**b** and **2a**,**b**; nevertheless the anti-HIV-1 activity in MT-4 cells of these four compounds is of the same order of magnitude (Table 5). However, one has to consider that total CEM cell extract is an oversimplified model of intracellular medium and that kinetics of uptake are not taken into account in the present study.

Conclusion

We have firmly established the decomposition pathways of compounds of types II and III which lead to intracellular isoddAMP delivery in cell extract, and this is corroborated by their HIV inhibitory effect in cell culture.

The observed mechanisms of decomposition may give insights into the design of new pronucleotides. For carboxyesterase-activated compounds, the initial enzyme-mediated hydrolytic attack must be preferentially directed to the electrophilic carbonyl center rather than to the electrophilic phosphorus atom in order to avoid any eventual carboxyesterase inhibition. This makes the choice of the leaving group for type III compounds of critical importance. In this respect one can hypothesize that a selective C−O activating bond breakage process is to be prefered over the P−O one in the conception of new classes of bioreversible phosphate protecting groups.

The biological consequences of NuMP delivery, thus bypassing the highly regulated and selective nucleoside first kinase, are numerous and will depend on each nucleoside metabolism, the prerequisite being that the corresponding NuTP is a viral polymerase inhibitor. In this respect, we have already reported that, when applied to ddA, the SATE approach leads to a more potent HIV inhibitor than AZT.[6] Also, and at the opposite of the parent nucleoside acyclovir (ACV), the corresponding bis(SATE)ACVMP derivatives show potent anti-HBV activities in cell culture systems.[17] Obviously the pronucleotide approach merits further evaluation for *in vivo* consequences. Work along this line is in progress in our laboratory.

Experimental Section

Chemical Synthesis. Evaporation of solvents was carried out on a rotary evaporator under reduced pressure. Melting points were determined on a Buchi SMP-20 apparatus and are uncorrected. ^{1}H NMR spectra were run at ambient temperature in $(CD_3)_2SO$ or $CDCl_3$ with a Bruker AC 250 spectrometer. Chemical shifts are given in δ values, $(CD_3)(CD_2H)SO$ being set at δ_H 2.49 as reference, and for $CDCl_3$, tetramethylsilane was used as the internal reference. Deuterium exchange and decoupling experiments were performed in order to confirm proton assignments. ^{31}P NMR spectra were recorded at ambient temperature on a Bruker AC 250 spectrometer with proton decoupling. Chemical shifts are reported relative to external H_3PO_4. FAB mass spectra were recorded in the positive-ion or negative-ion mode on a JEOL DX 300 mass spectrometer operating with a JMA-DA 5000 mass data system. Xe atoms were used for the gun at 3 kV with a total discharge current of 20 mA. The matrix used was a mixture (50:50, v/v) of glycerol and thioglycerol (G−T). UV spectra were recorded on an Uvikon 810 (Kontron) spectrometer. TLC was performed on precoated aluminium sheets of silica gel 60 F_{254} (Merck, Art. 5554), visualization of products being accomplished by UV absorbance followed by charring with 10% ethanolic sulfuric acid with heating; phosphorus-containing compounds were detected by spraying with Hanes molybdate reagent.[18] Column chromatography was carried out on silica gel 60 (Merck, Art. 9385) at atmospheric pressure. High-performance liquid chromatography (HPLC) purity tests were carried out on a Waters Associates Unit (Waters, Milford, MA) equipped with a model 600E multisolvent delivery system, a model 600E system controller, a model U6K sample injector, a model 486 tunable absorbance detector, and a Baseline 810 data workstation. The analytical column (Hypersil ODS, 100 × 4.6 mm, 3 μm, Life Sciences International, Eragny, France) was protected by a prefilter and a precolumn (Guard Pak, Resolve C_{18}, Waters). The compounds to be analyzed were eluted using a linear gradient from 0 to 50% acetonitrile in 0.1 M ammonium acetate buffer pH 5.9, programmed over a 60 min period with a flow rate of 1 mL/min and detection at 260 nm.

IsoddA-5′-(phenyl methoxyalaninylphosphate) (1a). The title compound was obtained as previously described.[9]

IsoddA-5′-(*p*-nitrophenyl methoxyalaninylphosphate) (1b). This compound was obtained adapting a published

procedure.[8b] IsoddA (0.3 g, 1.3 mmol) was added to a stirred solution of *p*-nitrophenylmethoxyalaninyl phosphorochloridate (3.5 mmol) (prepared from L-alanine methyl ester hydrochloride and *p*-nitrophenyl phosphorodichloridate) and *N*-methylimidazole in tetrahydrofuran (10 mL). After 2 h at room temperature, the solvent was removed under reduced pressure. The residual oil was dissolved in chloroform (20 mL) and washed with a 1 M solution of hydrochloride acid (2 × 10 mL), satured sodium bicarbonate solution (2 × 10 mL), and then water (2 × 10 mL). The organic phase was dried over sodium sulfate and evaporated to dryness. The residue was taken up in the minimum amount of chloroform and chromatographed on a silica gel column using methanol (4%) in chloroform as eluent. Yield: 274 mg (45%) of light yellow solid. Mp: 140 °C. UV (EtOH 95): λ_{max} = 262 nm (ϵ 18 800). ^{1}H NMR ($CDCl_3$): δ (peaks labeled with an asterisk are duplicated due to diastereoisomers) 1.41* (d, J = 7.1 Hz, 3H, Ala-Me), 2.15 and 2.70 (2m, 2H, H-3′), 3.70* (s, 3H, OMe), 3.85 (m, 1H, NH), 4.0−4.40 (m, 6H, Ala-CH, H-2′, Ha-5′, Hb-5′, and CH_2OP), 5.30 (m, 1H, H-4′), 5.60 (br s, 2H, NH_2), 7.40* (d, J = 9.1 Hz, 2H, Ph), 8.05* (s, 1H, H-2), 8.20* (d, J = 9.1 Hz, 2H, Ph), 8.35* (s, 1H, H-8). ^{31}P NMR ($CDCl_3$): δ 3.15, 2.83 (4:3). MS (FAB > 0): m/z 522 $[M + H]^+$. MS (FAB < 0): m/z 520 $[M - H]^-$. HPLC: t_R 41.9, 43.4 min. Anal. ($C_{20}H_{24}N_7O_8P$) C, H, N.

IsoddA-5′-(methoxyalaninylphosphoramidate) Triethylammonium Salt (3). Compound **1b** (50 mg, 0.096 mmol) was dissolved in a solution of triethylamine (3 mL) and water (0.1 mL). The mixture was stirred at room temperature for 1.5 h and then evaporated to dryness under reduced pressure. The residue was purified by chromatography on silica gel column using water (20%) in acetonitrile. Yield: 33.6 mg (70%) of a colorless solid which was crystallized from diethyl ether containing few drops of methanol. Mp: 190−192 °C. UV (EtOH 95): λ_{max} = 259 nm (ϵ 15 300). ^{1}H NMR (D_2O): δ 1.21 (pseudo t, 12H, CH_3CH$_2$ and Ala-Me), 2.06, 2.70 (2m, 2H, H-3′), 3.36 (q, 6H, CH$_3$CH_2), 3.55 (s, 3H, OCH$_3$), 3.58 and 3.78 (2m, 2H, CH_2OP), 3.83−4.29 (m, 4H, Ha-5′, Hb-5′, H-2′, and Ala-CH), 5.16 (m, 1H, H-4′), 8.11 (s, 1H, H-2); 8.23 (s, 1H, H-8). ^{31}P NMR (D_2O): δ 7.04. MS (FAB > 0): m/z 401 $[M + H]^+$. MS (FAB < 0): m/z 399 $[M - H]^-$. HPLC: t_R 29.4 min. Anal ($C_{20}H_{36}N_7O_6P$) C, H, N.

IsoddA-5′-(alaninylphosphoramidate) Triethylammonium Salt (4). Compound **1b** (50 mg, 0.096 mmol) was dissolved in a solution of triethylamine (2.5 mL) and water (2.5 mL). The mixture was stirred at 40 °C for 2 h and then evaporated to dryness under reduced pressure. The residue was treated with water (5 mL) and extracted with diethyl ether (4 × 15 mL). The aqueous layer was evaporated under reduced pressure to give the crude product which was crystallized from diethyl ether containing few drops of methanol. Yield: 37.3 mg (80%). Mp: 210−212 °C. UV (EtOH 95): λ_{max} = 259 nm (ϵ 14 200). ^{1}H NMR (D_2O): δ 1.20 (pseudo t, 12H, CH_3CH$_2$ and Ala-Me), 2.10 and 2.70 (2m, 2H, H-3′), 3.10 (q, 6H, CH$_3$CH_2), 3.55 and 3.82 (2m, 2H, CH_2OP), 3.90−4.30 (m, 4H, Ha-5′, Hb-5′, H-2′, and Ala-CH), 5.22 (m, 1H, H-4′), 8.21 (s, 1H, H-2), 8.35 (s,1H, H-8). ^{31}P NMR (D_2O): δ 7.56. MS (FAB > 0): m/z 387 $[M + H]^+$. MS (FAB < 0): m/z 385 $[M - H]^-$. HPLC t_R 8.4 min. Anal. ($C_{19}H_{34}N_7O_6P$) C, H, N.

General Procedure for the Preparation of the Bis-(SATE) Phosphotriesters (2a,b). Adapting a published procedure,[6] 1*H*-tetrazole (42 mg, 0.60 mmol) was added to a stirred solution of isoddA (47 mg, 0.20 mmol) and the appropriate phosphoramidite (0.24 mmol) (prepared from (*S*)-2-hydroxyethylthioacylate and *N*,*N*-diisopropylphosphorodichloridite[6]) in a mixture of tetrahydrofuran (0.80 mL) and *N*,*N*-dimethylformamide (1.0 mL). After 35 min at room temperature, the reaction mixture was cooled to −40 °C and a 3 M solution of *tert*-butyl hydroperoxide in toluene (0.16 mL, 0.48 mmol) was added. The solution was then allowed to reach room temperature over 1 h, and chloroform (10 mL) was added. Sodium hydrogen sulfite (10% aqueous solution, 1 mL) was added to reduce the excess of *tert*-butyl hydroperoxide. The organic layer was separated, washed with water (2 × 1 mL), dried over sodium sulfate, and evaporated to dryness. The residue was taken up in the minimum amount of methylene chloride and chromatographed on a silica gel column using a gradient of methanol (0−4%) in methylene chloride.

IsoddA-5′-[bis(*S*-acetyl-2-thioethyl)]phosphate (2a). Yield: 60 mg (58%). UV (EtOH 95): λ_{max} 259 (ϵ 13 700). ^{1}H NMR (DMSO-d_6): δ 2.13 (m, 1 H, H-3″), 2.33 (s, 6 H, CH$_3$-CO), 2.65 (m, 1 H, H-3′), 3.12 and 3.13 (2t, J = 6.3 Hz, 4 H, CH$_2$CH_2S), 3.99−4.20 (m, 9 H, H-2′, H-5′, H-5″, OCH_2CH$_2$), 5.18 (m, 1 H, H-4′), 7.27 (s, 2 H, NH_2), 8.14 and 8.17 (2s, 2 H, H-2 and H-8). ^{31}P NMR (DMSO-d_6): δ −0.74. MS (FAB > 0): m/z 520 $[M + H]^+$, 103 $[CH_3C(O)SCH_2CH_2]^+$.

IsoddA-5′-[bis(*S*-pivaloyl-2-thioethyl)]phosphate (2b). Yield: 96 mg (80%). UV (EtOH 95): λ_{max} 259 (ϵ 12 800). ^{1}H NMR (DMSO-d_6): δ 1.16 (s, 18 H, $(CH_3)_3$C), 2.14 (m, 1 H, H-3″), 2.62 (m, 1 H, H-3′), 3.10 and 3.11 (2t, J = 6.3 Hz, 4 H, CH$_2$CH_2S), 3.98−4.24 (m, 9 H, H-2′, H-5′, H-5″, OCH_2CH$_2$), 5.17 (m, 1 H, H-4′), 7.17 (s, 2 H, NH_2), 8.12 and 8.15 (2s, 2 H, H-2 and H-8). ^{31}P NMR (DMSO-d_6): δ −0.74. MS (FAB > 0): m/z 604 $[M + H]^+$, 145 $[(CH_3)_3C(O)SCH_2CH_2]^+$.

Antiviral Assay Procedures. Activity of the compounds against HIV-1 (III_B strain) and HIV-2 (CBL-20 strain) multiplication in acutely infected cells was based on the inhibition of virus-induced cytopathogenicity in MT-4 and C8166 cells, respectively. Briefly, 50 μL of culture medium containing 1 × 10^4 cells was added to each well of flat-bottomed microtitre trays containing 50 μL of culture medium with or without various concentrations of the test compounds. Then, 20 μL of an HIV suspension containing 100 (HIV-1) or 1000 (HIV-2) CCID50 (50% cell culture infective dose) was added. After a 4-day incubation at 37 °C, the number of viable cells was determined by the 3-(4,5-dimethylthiazol-1-yl)-2,5-diphenyltetrazolium bromide (MTT) method. Cytotoxicity of the compounds was evaluated in parallel with their antiviral activity. It was based on the viability of mock-infected cells, as monitored by the MTT method.

Stability Studies. The general procedure was as previously described,[7] and the HPLC analysis was recently improved.[4] HPLC instrumentation included a Waters LC System (Model 717$^+$ autosampler, Model 616 pump with column heater and controller 600S, Model 996 photodiode array detector) coupled to a Millenium Chromatography Manager System (Waters, Milford, MA), which also controlled the two automated switching valves (Phase Sep, Pessac, France). When using the "on-line" cleaning method without ion-pairing reagent, the retention times (min) of analytes were as follows (ca.): **1a**, 33.3 and 34.6; **1b**, 34.1 and 36.6; **2a**, 35.2; **2b**, 43.8; **3**, 18.6; **9**, 16.7; **11a**, 27.5; **11b**, 29.2; **12**, 25.5; **14a**, 24.3; **4** and **8**, <4 min (column thermostated at 30 °C). When using the method with ion-pairing reagent, all the retention times were close to the preceeding values except for the following: **4**, 15.1; **8**, 14.1; **3**, 19.6; and **9**, <4 min. The relative concentration of each component was calculated from the areas at 260 nm of the corresponding signals. Data for compounds **2a**,**b** were treated as previously described for their AZT analogs.[4] Calculations were complicated in the cases of compounds **1a,b** because the sum of areas of all the signals (at 260 nm) was not constant during the course of the experiments. This is due to the fact that the UV spectrum in the HPLC eluent of the starting compound (e.g. λ_{max} = 263 nm with a shoulder at 292 nm for the two diastereoisomers of **1b**) is different to those of the metabolites which lack the aromatic chromophore (**3**, **4**, **8**, and **9**, λ_{max} = 260 nm) and is not the envelope of the spectra corresponding to these metabolites and to the *p*-nitrophenol (λ_{max} = 226 and 319 nm). The increase of the absorption coefficient of aryl phosphoramidate derivatives **1a**,**b** as compared to the sum of absorption coefficients corresponding to the aryl and nucleoside moieties was confirmed when incubating compound **1b** in the presence of pig liver carboxyesterases in the cell of a spectrophotometer: the absorbance at 260 nm decreased in 1 h to ca. 80% of its initial value and then plateaued. Therefore the relative concentrations of all compounds could be calculated from HPLC data when assuming that ϵ(**9**) = ϵ(**8**) = ϵ(**4**) = ϵ(**3**) and introducing a correcting factor ϵ(**9**)/ϵ(**1**) in the Beer−Lambert rule. This factor was statistically optimized so that the sum of the corrected areas at 260 nm (hence of concentrations) was constant whatever the incubation time. Reproducible values of this ratio were found in all HPLC experiments, respectively 0.77 for **1a** and 0.75 for **1b**, which proves the validity of these assumptions (the last ratio is in good accordance with those found for **1b**,**3**,**4**

in EtOH 95; see the Chemical Synthesis Section). Rate constants of each step were optimized by a least-square regression (SigmaPlot software, Jandel, Erkrath, Germany) corresponding to integrated equations (Scheme 5). Equations were established according to the overall decomposition scheme (competitive−consecutive pseudo-first-order), taking into account that the investigated sample **1** may be either pure or mixed with compound **3**.

HPLC/MS Coupling. Compound **1b** (25 μM) was incubated either 5 h in the full cell extract or 10 h in the culture medium, and then the incubates were pooled and 100 μL were injected in a system composed of the cleaning device, a TSP chromatograph 4100MS with UV detection at 260 nm, and a mass spectrometer SSQ 7000 (Finnigan Mat, Orsay, France). After elimination of proteins, the cleaning precolumn was connected to the analytical column, the UV detector was connected to the mass spectrometer, and the whole eluting flow (1 mL/min) was both UV and MS analyzed. According to the cleaning conditions (ion-pairing method), all components could be analyzed except the nucleoside **9**. The best MS conditions were found when using the negative electrospray mode. The observed masses were (calculated M, found $[M - H]^-$) as follows: **1b** (521.14; 520.1); **3** (400.13; 399.1); **4** (386.11; 385.1); **8** (315.07; 314.0). In the collision mode, a fragment at m/z = 339.1 was observed, either from signal **3** ($[M - HCOOCH_3 - H]^-$) or signal **4** ($[M - HCOOH - H]^-$), thus proving the structure of the last component.

Similarly, compound **2a** was incubated 2 h in the full cell extract, and 100 μL was injected in the system. Results were (calculated M, found $[M - H]^-$) as follows: **2a** (519.1; 518.0); **11a** (417.1; 416.0); **12** (375.1; 374.0); **14a** (357.1; 356.0); **8** (315.07; 314.0).

In another experiment, a reconstituted aqueous mixture of authentic samples **1b**, **3**, **4**, **8**, and **9** (100−200 μM each) was directly injected (20 μL) in the analytical column, then chromatographed, and analyzed in a similar apparatus but using a VG-Platform Mass spectrometer (Fisons instruments SA, Arcueil, France). Only one twentieth of the eluate (20-fold splitting, flow rate 50 μL/min) was allowed to enter into the mass spectrometer. Results were quite similar to those aforementioned. It is to be noted that the isoddA nucleoside **9** was undetectable in the negative electrospray mode but was detectable in the positive mode (calculated mass 235.1, found 235.9 $[M + H]^+$).

Acknowledgment. This investigation was supported by grants from Agence Nationale de Recherches sur le Sida (ANRS), Association pour la Recherche sur le Cancer (ARC), Centre National de la Recherche Scientifique (CNRS), and Ministero della Sanità, Istituto Superiore di Sanità (Grants 9204-62, progetto AIDS 1994, and 9304-75, progetto AIDS 1995). We thank Dr. A.-M. Aubertin (Strasbourg, France) for the preparation of cell extracts and the Centre Régional de Transfusion Sanguine (Montpellier, France) for generous gift of human blood samples from healthy volunteers. We acknowledge Dr. E. Roselier (Fisons Instrument SA, Arcueil, France) and Dr. E. Génin (Finnigan Mat, Orsay, France) for preliminary HPLC/MS coupling experiments. We are indebted to Dr. R. Johnson for critical reading of the manuscript.

References

(1) (a) Périgaud, C.; Girardet, J.-L.; Gosselin, G.; Imbach, J.-L. Comments on nucleotide delivery forms. In *Advances in Antiviral Drug Design*; De Clercq, E., Ed., 1995; Vol. 2, pp 167−172. (b) Alexander, P.; Holy, A. Prodrugs of analogs of nucleic acid components. *Collect. Czech. Chem. Commun.* **1994**, *59*, 2127−2165. (c) Jones, R. J.; Bischofberger, N. Nucleotide prodrugs. *Antiviral Res.* **1995**, *27*, 1−17.

(2) Sommadossi, J. P. Nucleoside analogs: similarities and differences. *Clin. Infect. Diseases* **1993**, *16* , S7−S15.

(3) (a) Sastry, K. J.; Nehete, P. N.; Khan, S.; Plunkett, W.; Arlinghaus, R. B.; Farquhar, D. A new strategy for the chemotherapy of acquired immune immunodeficiency syndrome: membrane permeable dideoxyuridine monophosphate analogues as potent inhibitors of human immunodeficiency virus infection. *Mol. Pharmacol.* **1992**, *41*, 441−445. (b) Srinivas, R. V.; Robbins, B. L.; Connelly, M. C.; Gong, Y.-F.; Bischofberger, N.; Fridland, A. Metabolism and in vitro antiretroviral activities of bis-(pivaloyloxymethyl) prodrugs of acyclic nucleoside phosphonates. *Antimicrob. Agents Chemother.* **1993**, *37*, 2247−2250.

(4) Lefebvre, I.; Périgaud, C.; Pompon, A.; Aubertin, A.-M.; Girardet, J.-L.; Kirn, A.; Gosselin, G.; Imbach, J.-L. Mononucleoside phosphotriester derivatives with bioreversible S-acyl-2-thioethyl phosphate protecting groups. Intracellular delivery of 3′-azido-2′,3′-dideoxythymidine 5′-monophosphate (AZTMP). *J. Med. Chem.* **1995**, *38*, 3941−3950.

(5) Périgaud, C.; Gosselin, G.; Lefebvre, I.; Girardet, J.-L.; Benzaria, S.; Barber, I.; Imbach, J.-L. Rational design for cytosolic delivery of nucleoside monophosphates: "SATE" and "DTE" as enzyme-labile transient phosphate protecting groups. *Bioorg. Med. Chem. Lett.* **1993**, *3*, 2521−2526.

(6) (a) Périgaud, C.; Aubertin, A.-M.; Benzaria, S.; Pelicano, H.; Girardet, J.-L; Maury, G.; Gosselin, G.; Kirn, A.; Imbach, J.-L. Equal inhibition of the replication of human immunodeficiency virus in human T-cell culture by ddA bis(SATE)phosphotriester and 3′-azido-2′,3′-dideoxythymidine. *Biochem. Pharmacol.* **1994**, *48*, 11−14. (b) Benzaria, S.; Girardet, J.-L; Périgaud, C.; Aubertin, A.-M.; Pelicano, H.; Maury, G.; Gosselin, G.; Kirn, A.; Imbach, J.-L. The SATE pronucleotide derivative of ddA: a more potent HIV inhibitor than AZT. *Nucleic Acids Symp. Series* **1994**, *31*, 129−130.

(7) Pompon, A.; Lefebvre, I.; Imbach, J.-L.; Kahn, S.; Farquhar, D. Decomposition pathways of the mono- and bis(pivaloyloxymethyl) esters of azidothymidine 5′-monophosphate in cell extract and in tissue culture medium: an application of the "on-line ISRP-cleaning" HPLC technique. *Antiviral Chem. Chemother.* **1994**, *5*, 91−98.

(8) (a) McGuigan, C.; Pathirana, R. N.; Balzarini, J.; De Clercq, E. Intracellular delivery of bioactive AZT nucleotides by aryl phosphate derivatives of AZT. *J. Med. Chem.* **1993**, 36, 1048−1052. (b) McGuigan, C.; Pathirana, R. N.; Mahmood, N.; Devine, K. G.; Hay, A. J. Aryl phosphate derivatives of AZT retain activity against HIV1 in cell lines which are resistant to the action of AZT. *Antiviral Res.* **1992**, *17*, 311−321.

(9) Franchetti, P.; Cappellacci, L.; Grifantini, M.; Messini, L.; Abu Sheikha, G.; Loi, A. G.; Tramontano, E.; De Montis, A.; Spiga, M. G.; La Colla, P. Synthesis and evaluation of the anti-HIV activity of aza and deaza analogues of isoddA and their phosphates as prodrugs. *J. Med. Chem.* **1994**, 37, 3534−3541.

(10) Shabarova, Z.; Bogdanov, A. In *Advanced Organic Chemistry of Nucleic Acids*; VCH Publishers, Inc.: New York, 1994; pp 93−180.

(11) Heymann, E. Carboxylesterases and Amidases. In *Enzymatic Basis of Detoxification. Biochemical Pharmacology and Toxicology Series Vol II*; Jacoby, W. B., Bend, R. R., Eds.; Academic Press: New York, 1980; pp 291−323.

(12) Satoh, T. Role of carboxylesterases in xenobiotic metabolism. *Rev. Biochem. Toxicol.* **1987**, *8*, 155−181.

(13) Aldridge, W.; Reiner, E. *Enzyme Inhibitors as Substrates: Interaction of esterases with esters of organophosphorus and carbamic acids*; North-Holland Publishing Co.: Amsterdam, 1972.

(14) Berman, H. A.; Leonard, K. Chiral reactions of acetylcholinesterase probed with enantiomeric methylphosphonothioates. *J. Biol. Chem.* **1989**, *264*, 3942−3950.

(15) Zhao, Q.; Kovach, I. M.; Bencsura, A.; Papathanassiu, A. Enantioselective and reversible inhibition of trypsin and α-chymotrypsin by phosphonate esters. *Biochemistry* **1994**, *33*, 8128−8138.

(16) Mutschler, E. M. D.; Derendorf, H.; Schäfer-Korting, M.; Elrod, K.; Estes, K. S. *Drug Actions*, Medpharm ed.; Stuttgart, 1995; pp 512−514.

(17) Gosselin, G.; Girardet, J.-L.; Périgaud, C.; Benzaria, S.; Lefebvre, I.; Schlienger, N.; Pompon, A; Imbach, J.-L. New insights regarding the potential of the pronucleotide approach in antiviral chemotherapy. *Acta Biochim. Polonica*, in press.

(18) Hanes, C. S.; Isherwood, F. A. Separation of the phosphoric esters on the filter paper chomatogram. *Nature* **1949**, *154*, 1107−1112.

JM9507338